We are IntechOpen, the world's leading publisher of Open Access books Built by scientists, for scientists

4,800
Open access books available

122,000
International authors and editors

135M
Downloads

Our authors are among the

154
Countries delivered to

TOP 1%
most cited scientists

12.2%
Contributors from top 500 universities

CLARIVATE ANALYTICS BOOK CITATION INDEX INDEXED

WEB OF SCIENCE™

Selection of our books indexed in the Book Citation Index in Web of Science™ Core Collection (BKCI)

Interested in publishing with us?
Contact book.department@intechopen.com

Numbers displayed above are based on latest data collected.
For more information visit www.intechopen.com

2

Golden Ratio in the Point Sink Induced Consolidation Settlement of a Poroelastic Half Space

Feng-Tsai Lin[1] and John C.-C. Lu[2]
[1]*Department of Naval Architecture, National Kaohsiung Marine University*
[2]*Department of Civil Engineering & Engineering Informatics, Chung Hua University*
Taiwan

1. Introduction

The golden ratio ϕ has been well known in mathematics, science, biology, art, architecture, nature and beyond (Sen & Agarwal, 2008), which is the irrational algebraic number $\left(1+\sqrt{5}\right)\Big/2 \approx 1.618033989$. It's interesting to find that the golden ratio exists in the point sink induced consolidation settlement of a homogeneous isotropic poroelastic half space. Examples of the golden ratio in engineering include the study of shear flow in porous half space (Puri & Jordan, 2006) and classical mechanics of coupled-oscillator problem (Moorman & Goff, 2007).

Land subsidence due to groundwater withdrawal is a well-known phenomenon (Poland, 1984). The pore water pressure is reduced in the withdrawal region when an aquifer pumps groundwater. It leads to increase in effective stress between the soil particles and subsidence of ground surface.

The three-dimensional consolidation theory presented by Biot (1941, 1955) is generally regarded as the fundamental theory for modeling land subsidence. Based on Biot's theory, Booker and Carter (1986*a*, 1986*b*, 1987*a*, 1987*b*), Kanok-Nukulchai and Chau (1990), Tarn and Lu (1991) presented solutions of subsidence by a point sink embedded in saturated elastic half space at a constant rate. In the studies of Booker and Carter (1986*a*, 1986*b*, 1987*a*, 1987*b*), the flow properties are considered as isotropic or cross-anisotropic whereas the elastic properties of the soil are treated as isotropic with pervious half space boundary. Tarn and Lu (1991) found that groundwater withdrawal from an impervious half space induces a larger amount of consolidation settlement than from a pervious one. Chen (2002, 2005) presented analytical solutions for the steady-state response of displacements and stresses in a half space subjected to a point sink. Lu and Lin (2006) displayed transient ground surface displacement produced by a point heat source/sink through analog quantities between poroelasticity and thermoelasticity. Hou *et al.* (2005) found that pumping induced ground horizontal velocities range from 31 to 54 mm/yr towards azimuths 247° to 273° in the Pingtung Plain of Taiwan. Their results show that ground horizontal displacement occurred

when pumping from an aquifer. Nevertheless, the consolidation settlement due to pumping were not thoroughly discussed in the above theoretical studies.
The aquifer is modeled as an isotropic saturated pervious elastic half space in this analytical research. Using Laplace and Hankel integral transform techniques, the transient horizontal and vertical displacements of the ground surface due to a point sink are obtained. The study also focused on the distributions of excess pore water pressure of the half space on the consolidation history. Results are illustrated and compared to display the time dependent consolidation settlement due to pumping.

2. The Golden Ratio

The golden ratio ϕ can be derived from a geometrical line segment in extreme and mean ratio as shown in Fiqure 1, where the ratio of the full length 1 to the length of x is equal to the ratio of section part x to shorter section $1-x$:

$$\frac{1}{x}=\frac{x}{1-x}. \tag{1}$$

Assuming, $x=1/\phi$, hence, ϕ satisfies

$$\phi^2-\phi-1=0. \tag{2}$$

The golden ratio is the positive root of Eq. (2):

$$\phi=\frac{1+\sqrt{5}}{2}. \tag{3}$$

Fig. 1. Dividing the unit interval according to the golden ratio

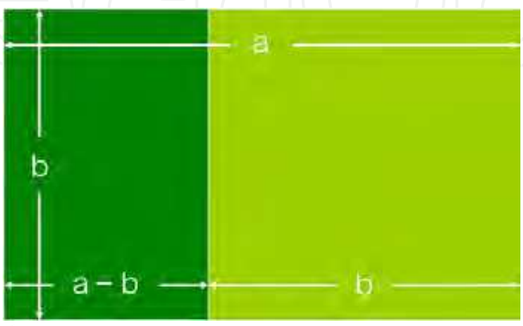

Fig. 2. The golden rectangle

Ratio of two successive numbers of Fibonacci series	Value
1/1	1.0000000000
2/1	2.0000000000
3/2	1.5000000000
5/3	1.6666666667
8/5	1.6000000000
13/8	1.6250000000
21/13	1.6153846154
34/21	1.6190476190
55/34	1.6176470588
89/55	1.6181818182
144/89	1.6179775281
233/144	1.6180555556

Table 1. The ratio of two successive numbers of Fibonacci series approaches golden ratio ϕ

Figure 2 displayed another geometric description of golden ratio through the golden rectangle. Giving a rectangle with sides' ratio a : b, the removing of square section leaves the remaining rectangle with the same ratio as original rectangle, i.e.,

$$\frac{b}{a-b}=\frac{a}{b}. \tag{4}$$

Thus, this solution is the golden ratio ϕ :

$$\phi=\frac{a}{b}=\frac{1+\sqrt{5}}{2}. \tag{5}$$

The golden ratio is a remarkable number that arises in various areas of mathematics, natures and arts. There are many interesting mathematical properties of ϕ . For example, ϕ can be expressed as a continuous fraction with the single number 1 (Livio, 2002):

$$\phi=1+\cfrac{1}{1+\cfrac{1}{1+\cfrac{1}{1+\cfrac{1}{1+\cdots}}}}. \tag{6}$$

Also, the golden ratio ϕ can be expressed as a continuous square root of the number 1:

$$\phi=\sqrt{1+\sqrt{1+\sqrt{1+\sqrt{1+\cdots}}}}. \tag{7}$$

However, the most interesting is that ϕ is within Fibonacci series (Livio, 2002; Dunlap, 1997). The Fibonacci series is a set of numbers that begins with two 1s and each term therefore is the sum of the prior two terms, i.e., 1, 1, 2, 3, 5, 8, 13, 21, 34, 55, 89, 144, 233, ⋯ . The relationship between two successive numbers of Fibonacci series tends to approach ϕ as shown in Table 1.

Based on Biot's (1941, 1955) three-dimensional consolidation theory of porous media, this study modeled the saturated aquifer as a homogeneous isotropic poroelastic half space. Closed-form solutions of the transient and long-term consolidation deformations and excess pore water pressures due to a point sink are presented in this paper. It's interesting to find that the golden ratio ϕ appears in the point sink induced maximum ground surface horizontal displacement and corresponding settlement of a poroelastic half space.

3. Mathematical Models

3.1 Basic Equations

Figure 3 presents a point sink buried in a saturated porous elastic aquifer at a depth h . The aquifer is considered as a homogeneous isotropic porous medium with a vertical axis of symmetry. Assuming the model is decoupled, i.e., the flow field is independent from the displacement field. Considering a point sink of constant strength Q located at point $(0,h)$, the basic governing equations of the elastic saturated aquifer for linear axially symmetric deformation can be expressed in terms of displacements u_i and excess pore water pressure p in the cylindrical coordinates (r,θ,z) as follows (Lu & Lin, 2006, 2008):

$$G\nabla^2 u_r + \frac{G}{1-2\nu}\frac{\partial \varepsilon}{\partial r} - G\frac{u_r}{r^2} - \frac{\partial p}{\partial r} = 0\,, \tag{8a}$$

$$G\nabla^2 u_z + \frac{G}{1-2\nu}\frac{\partial \varepsilon}{\partial z} - \frac{\partial p}{\partial z} = 0\,, \tag{8b}$$

$$-\frac{k}{\gamma_w}\nabla^2 p + n\beta\frac{\partial p}{\partial t} + \frac{Q}{2\pi r}\delta(r)\delta(z-h)u(t) = 0\,, \tag{8c}$$

where $\nabla^2 = \partial^2/\partial r^2 + 1/r\,\partial/\partial r + \partial^2/\partial z^2$ is the Laplacian operator. The excess pore fluid pressure p is positive for compression. The displacements u_r and u_z are in the radial and axial directions, and $\varepsilon = \partial u_r/\partial r + u_r/r + \partial u_z/\partial z$ is the volume strain of the porous medium. The quantities ν , G , k , n , γ_w and β denote the saturated aquifer's Poisson's ratio, shear modulus, aquifer permeability, porosity, pore water unit weight and compressibility, respectively. The functions $\delta(x)$ and $u(t)$ are Dirac delta and Heaviside unit step function, respectively.

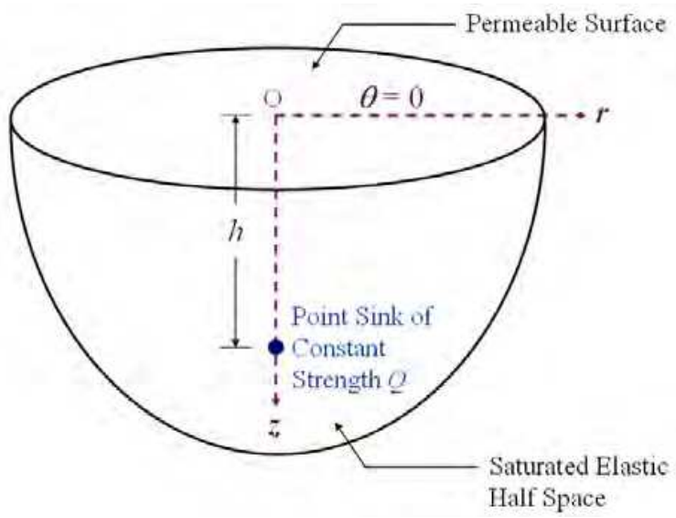

Fig. 3. Point sink induced land subsidence model

3.2 Boundary Conditions

The saturated aquifer is considered as a homogeneous isotropic half space and the constitutive behavior of the aquifer can be express by the total stress components $\tau_{ij} = \frac{2G\nu}{1-2\nu}\varepsilon\delta_{ij} + 2G\varepsilon_{ij} - p\delta_{ij}$, where $\varepsilon_{rr} = \frac{\partial u_r}{\partial r}$, $\varepsilon_{\theta\theta} = \frac{u_r}{r}$, $\varepsilon_{zz} = \frac{\partial u_z}{\partial z}$, respectively; and δ_{ij} is the Kronecker delta. In this paper, the half space surface, $z = 0$, is considered as a traction-free pervious boundary for time $t \geq 0$. From the constitutive relationships shown above, the mechanical boundary conditions at $z = 0$ are expressed in terms of u_r and u_z by

$$\frac{2G\nu}{1-2\nu}\left[\frac{\partial u_r(r,0,t)}{\partial r} + \frac{u_r(r,0,t)}{r}\right] + \frac{2G(1-\nu)}{1-2\nu}\frac{\partial u_z(r,0,t)}{\partial z} = 0, \tag{9a}$$

$$G\left[\frac{\partial u_r(r,0,t)}{\partial z} + \frac{\partial u_z(r,0,t)}{\partial r}\right] = 0. \tag{9b}$$

An additional condition is provided by considering the half space as pervious and the mathematical statement of the flow condition at the boundary $z = 0$ is given by

$$p(r,0,t) = 0. \tag{9c}$$

The boundary conditions at $z \to \infty$ due to the effect of the point sink vanish when $t \geq 0$.

3.3 Initial Conditions

Assuming no initial changes in displacements and seepage of the aquifer, the initial conditions of the mathematical model at time $t = 0$ are

$$u_r(r,z,0) = 0,\ u_z(r,z,0) = 0, \text{ and } p(r,z,0) = 0. \tag{10}$$

4. Analytic Solutions

4.1 Laplace and Hankel Transforms Solutions

The governing partial differential equations (8a)-(8c) are reduced to ordinary differential equations by performing Laplace and Hankel transforms (Sneddon, 1951) with respect to the time variable t and the radial coordinate r :

$$\left(\frac{d^2}{dz^2}-2\eta\xi^2\right)\tilde{u}_r-(2\eta-1)\xi\frac{d\tilde{u}_z}{dz}+\frac{1}{G}\xi\tilde{p}=0\,, \tag{11a}$$

$$(2\eta-1)\xi\frac{d\tilde{u}_r}{dz}+\left(2\eta\frac{d^2}{dz^2}-\xi^2\right)\tilde{u}_z-\frac{1}{G}\frac{d\tilde{p}}{dz}=0\,, \tag{11b}$$

$$-\frac{k}{\gamma_w}\left(\frac{d^2}{dz^2}-\xi^2\right)\tilde{p}+n\beta s\tilde{p}+\frac{Q}{2\pi s}\delta(z-h)=0\,, \tag{11c}$$

where ξ and s are Hankel and Laplace transform parameters. The parameter $\eta=(1-\nu)/(1-2\nu)$ and the symbols $\tilde{u}_r$, $\tilde{u}_z$, $\tilde{p}$ are defined as

$$\tilde{u}_r(z;\xi,s)=\int_0^\infty rL\{u_r(r,z,t)\}J_1(\xi r)dr\,, \tag{12a}$$

$$\tilde{u}_z(z;\xi,s)=\int_0^\infty rL\{u_z(r,z,t)\}J_0(\xi r)dr\,, \tag{12b}$$

$$\tilde{p}(z;\xi,s)=\int_0^\infty rL\{p(r,z,t)\}J_0(\xi r)dr\,, \tag{12c}$$

in which $J_\nu(x)$ represents the first kind of Bessel function of order ν . The Laplace transforms in equations (12a)-(12c) with respect to u_r, u_z and p are denoted by

$$L\{u_r(r,z,t)\}=\int_0^\infty u_r(r,z,t)exp(-st)dt\,, \tag{13a}$$

$$L\{u_z(r,z,t)\}=\int_0^\infty u_z(r,z,t)exp(-st)dt\,, \tag{13b}$$

$$L\{p(r,z,t)\}=\int_0^\infty p(r,z,t)exp(-st)dt\,. \tag{13c}$$

The general solutions of equations (11a)-(11c) are obtained as

$$\tilde{u}_r(z;\xi,s)=C_1exp(\xi z)+C_2z\,exp(\xi z)+C_3exp(-\xi z)+C_4z\,exp(-\xi z)$$
$$+C_5exp\left(\sqrt{\xi^2+\frac{s}{c}}z\right)+C_6exp\left(-\sqrt{\xi^2+\frac{s}{c}}z\right)$$

$$+\frac{Q\gamma_w}{8\pi\eta Gk}\left[-\frac{c}{s^2}exp\left(-\xi|z-h|\right)+\frac{c}{s^2}\frac{\xi}{\sqrt{\xi^2+\frac{s}{c}}}exp\left(-\sqrt{\xi^2+\frac{s}{c}}|z-h|\right)\right], \tag{14a}$$

$$\tilde{u}_z(z;\xi,s)=\left(-C_1+\frac{2\eta+1}{2\eta-1}\frac{1}{\xi}C_2\right)exp(\xi z)-C_2 z\,exp(\xi z)+\left(C_3+\frac{2\eta+1}{2\eta-1}\frac{1}{\xi}C_4\right)exp(-\xi z)+C_4 z\,exp(-\xi z)$$
$$-\frac{1}{\xi}\sqrt{\xi^2+\frac{s}{c}}C_5\,exp\left(\sqrt{\xi^2+\frac{s}{c}}z\right)+\frac{1}{\xi}\sqrt{\xi^2+\frac{s}{c}}C_6\,exp\left(-\sqrt{\xi^2+\frac{s}{c}}z\right)$$
$$\mp\frac{Q\gamma_w}{8\pi\eta Gk}\left[\frac{c}{s^2}exp\left(-\xi|z-h|\right)-\frac{c}{s^2}exp\left(-\sqrt{\xi^2+\frac{s}{c}}|z-h|\right)\right], \tag{14b}$$

$$\tilde{p}(z;\xi,s)=-2\eta G\frac{1}{\xi}\frac{s}{c}C_5\,exp\left(\sqrt{\xi^2+\frac{s}{c}}z\right)-2\eta G\frac{1}{\xi}\frac{s}{c}C_6\,exp\left(-\sqrt{\xi^2+\frac{s}{c}}z\right)$$
$$-\frac{Q\gamma_w}{4\pi k}\frac{1}{s}\frac{1}{\sqrt{\xi^2+\frac{s}{c}}}exp\left(-\sqrt{\xi^2+\frac{s}{c}}|z-h|\right), \tag{14c}$$

where the parameter $c=k/n\beta\gamma_w$ and $C_i\left(i=1,2,\cdots,6\right)$ are functions of the transformed variables ξ and s which are determined from the transformed boundary conditions. The upper and lower signs in Eq. (14b) are for the conditions of $(z-h)\geq 0$ and $(z-h)<0$, respectively.

4.2 Transformed Boundary Conditions

Taking Hankel and Laplace transforms for Eqs. (9a)-(9c), the mechanical and flow boundary conditions at $z=0$ of the transformed domains are derived as follows:

$$\eta\frac{d\tilde{u}_z(0;\xi,s)}{dz}+(\eta-1)\xi\tilde{u}_r(0;\xi,s)=0,\ \frac{d\tilde{u}_r(0;\xi,s)}{dz}-\xi\tilde{u}_z(0;\xi,s)=0,\ \text{and}\ \tilde{p}(0;\xi,s)=0, \tag{15}$$

where $\tilde{u}_r$, $\tilde{u}_z$ and $\tilde{p}$ follow the definitions in Eqs. (12a)-(12c).

The constants $C_i\left(i=1,2,\cdots,6\right)$ of the general solutions are determined by the transformed half space boundary conditions at $z=0$ and $z\to\infty$. Finally, the desired quantities u_r, u_z and p are obtained by applying appropriate inverse Hankel and Laplace transformations (Erdelyi, *et al.*, 1954).

4.3 Expressions for Ground Surface Displacements

The focus of the study is on horizontal and vertical displacements of the ground surface, $z=0$, due to a point sink. The transformed ground surface displacements are derived from Eqs. (14a)-(14b) with the help of transformed boundary conditions and they are obtained as follows:

$$\tilde{u}_r\left(0;\xi,s\right)=\frac{Q\gamma_w}{2\pi\left(2\eta-1\right)Gk}\left[-\frac{c}{s^2}exp\left(-\xi h\right)+\frac{c}{s^2}exp\left(-\sqrt{\xi^2+\frac{s}{c}}h\right)\right], \tag{16a}$$

$$\tilde{u}_z\left(0;\xi,s\right)=\frac{Q\gamma_w}{2\pi\left(2\eta-1\right)Gk}\left[\frac{c}{s^2}exp\left(-\xi h\right)-\frac{c}{s^2}exp\left(-\sqrt{\xi^2+\frac{s}{c}}h\right)\right]. \tag{16b}$$

Applying the Hankel inversion formulae lead to the following displacements:

$$u_r\left(r,z,t\right)=\int_0^\infty \xi L^{-1}\left\{\tilde{u}_r\left(z;\xi,s\right)\right\}J_1\left(\xi r\right)d\xi\,, \tag{17a}$$

$$u_z\left(r,z,t\right)=\int_0^\infty \xi L^{-1}\left\{\tilde{u}_z\left(z;\xi,s\right)\right\}J_0\left(\xi r\right)d\xi\,, \tag{17b}$$

in which the Laplace inversions are defined as

$$L^{-1}\left\{\tilde{u}_r\left(z;\xi,s\right)\right\}=\frac{1}{2\pi i}\int_{\alpha-i\infty}^{\alpha+i\infty}\tilde{u}_r\left(z;\xi,s\right)exp\left(st\right)ds\,, \tag{18a}$$

$$L^{-1}\left\{\tilde{u}_z\left(z;\xi,s\right)\right\}=\frac{1}{2\pi i}\int_{\alpha-i\infty}^{\alpha+i\infty}\tilde{u}_z\left(z;\xi,s\right)exp\left(st\right)ds\,. \tag{18b}$$

Using Eqs. (17a)-(17b) and (18a)-(18b), the transient horizontal displacement $u_r\left(r,0,t\right)$ and vertical settlement $u_z\left(r,0,t\right)$ of the pervious ground surface due to a point sink are obtained as follows:

$$u_r\left(r,0,t\right)=\frac{Q\gamma_w}{2\left(2\eta-1\right)\pi Gk}\left\{-\frac{ctr}{\left(h^2+r^2\right)^{3/2}}\right.$$
$$\left.+\int_0^{ct}\frac{\left(ct-\tau\right)hr}{16\tau^3}exp\left(-\frac{r^2+2h^2}{8\tau}\right)\left[I_0\left(\frac{r^2}{8\tau}\right)-I_1\left(\frac{r^2}{8\tau}\right)\right]d\tau\right\}, \tag{19a}$$

$$u_z\left(r,0,t\right)=\frac{Q\gamma_w}{2\left(2\eta-1\right)\pi Gk}\left\{\frac{cth}{\left(h^2+r^2\right)^{3/2}}erf\left(\frac{\sqrt{h^2+r^2}}{2\sqrt{ct}}\right)-\frac{h}{h^2+r^2}\sqrt{\frac{ct}{\pi}}exp\left(-\frac{h^2+r^2}{4ct}\right)\right.$$
$$\left.+\frac{h}{2\sqrt{h^2+r^2}}erfc\left(\frac{\sqrt{h^2+r^2}}{2\sqrt{ct}}\right)\right\}, \tag{19b}$$

where $erf\left(x\right)$ and $erfc\left(x\right)$ are error function and complementary error function, respectively; and $I_v\left(x\right)$ is known as the modified Bessel function of the first kind of order v. The long-term ground surface horizontal and vertical displacements are obtained when $t\to\infty$:

$$u_r(r,0,\infty) = -\frac{Q\gamma_w}{4(2\eta-1)\pi Gk}\frac{hr}{\sqrt{h^2+r^2}\left(\sqrt{h^2+r^2}+h\right)}, \tag{20a}$$

$$u_z(r,0,\infty) = \frac{Q\gamma_w}{4(2\eta-1)\pi Gk}\frac{h}{\sqrt{h^2+r^2}}. \tag{20b}$$

The maximum long-term ground surface horizontal displacement $u_{r\max}$ and settlement $u_{z\max}$ of the half space due to a point sink are derived from Eqs. (20a) and (20b) by letting $r=\sqrt{\phi}h \approx 1.272h$ and $r=0$, respectively:

$$u_{r\max} = u_r\left(\sqrt{\phi}h,0,\infty\right) = -\frac{Q\gamma_w}{4(2\eta-1)\pi Gk}\frac{1}{\phi^{2.5}} \approx -\frac{0.3003Q\gamma_w}{4(2\eta-1)\pi Gk}, \tag{21a}$$

$$u_{z\max} = u_z(0,0,\infty) = \frac{Q\gamma_w}{4(2\eta-1)\pi Gk}, \tag{21b}$$

in which $\phi=\left(1+\sqrt{5}\right)/2 \approx 1.618$ is known as the golden ratio (Livio, 2002; Dunlap, 1997). The value $r=\sqrt{\phi}h$ is derived when $du_r(r,0,\infty)/dr$ is equal to zero, i.e.,

$$\frac{du_r(r,0,\infty)}{dr} = -\frac{Q\gamma_w}{4(2\eta-1)\pi Gk}\frac{h\sqrt{h^2+r^2}\left(h^2-r^2\right)+h^4}{\left(h^2+r^2\right)^{1.5}\left(\sqrt{h^2+r^2}+h\right)^2} = 0. \tag{22}$$

This leads to solutions of $r=\pm\sqrt{(1+\sqrt{5})/2}h$ and $r=\pm\sqrt{(1-\sqrt{5})/2}h$, however only $r=\sqrt{(1+\sqrt{5})/2}h$ is realistic for $r\in[0,\infty)$.

It's interesting to find that the golden ratio ϕ not only appears in the point sink induced maximum ground surface horizontal displacement but also on the corresponding settlement by letting $r=\sqrt{\phi}h$ in Eq. (20b). Hence, we have:

$$u_z\left(\sqrt{\phi}h,0,\infty\right) = \frac{Q\gamma_w}{4(2\eta-1)\pi Gk}\frac{1}{\sqrt{1+\phi}} = u_{z\max}\frac{1}{\phi} \approx 0.618u_{z\max}. \tag{23}$$

This shows that the ground surface settlement at $r=\sqrt{\phi}h$, where the maximum ground surface horizontal displacement $u_{r\max}$ occurred, is around 61.8% of the maximum ground surface settlement $u_{z\max}$.

All of the displacement figures are normalized to the maximum ground surface settlement $u_{z\max}$. Besides, the Eqs. (21a)-(21b) show that the maximum long-term horizontal displacement and settlement are not directly dependent on the pumping depth h.

4.4 Expression for Excess Pore Water Pressure

The study also addressed the excess pore water pressure of the porous elastic half space due to a point sink. The transformed excess pore water pressure is obtained from Eq. (14c) with the help of transformed flow boundary conditions, and it can be expressed as following:

$$\tilde{p}\left(z;\xi,s\right)=\frac{Q\gamma_w}{4\pi k}\left\{\frac{1}{s}\frac{1}{\sqrt{\xi^2+\frac{s}{c}}}exp\left[-\sqrt{\xi^2+\frac{s}{c}}\left(z+h\right)\right]-\frac{1}{s}\frac{1}{\sqrt{\xi^2+\frac{s}{c}}}exp\left[-\sqrt{\xi^2+\frac{s}{c}}\left|z-h\right|\right]\right\}. \quad (24)$$

The Hankel inversion formula is applied as:

$$p\left(r,z,t\right)=\int_0^\infty \xi L^{-1}\left\{\tilde{p}\left(z;\xi,s\right)\right\}J_0\left(\xi r\right)d\xi\,, \quad (25)$$

where the Laplace inversion is defined as

$$L^{-1}\left\{\tilde{p}\left(z;\xi,s\right)\right\}=\frac{1}{2\pi i}\int_{\alpha-i\infty}^{\alpha+i\infty}\tilde{p}\left(z;\xi,s\right)exp\left(st\right)ds\,. \quad (26)$$

The transient excess pore water pressure $p\left(r,z,t\right)$ of the saturated pervious half space due to a point sink is obtained as following:

$$p\left(r,z,t\right)=\frac{Q\gamma_w}{4\pi k}\left\{\frac{1}{\sqrt{r^2+\left(z+h\right)^2}}erfc\left[\frac{\sqrt{r^2+\left(z+h\right)^2}}{2\sqrt{ct}}\right]-\frac{1}{\sqrt{r^2+\left(z-h\right)^2}}erfc\left[\frac{\sqrt{r^2+\left(z-h\right)^2}}{2\sqrt{ct}}\right]\right\}. \quad (27)$$

The long-term excess pore water pressure is derived when $t\to\infty$. It leads to

$$p\left(r,z,\infty\right)=\frac{Q\gamma_w}{4\pi k}\left[\frac{1}{\sqrt{r^2+\left(z+h\right)^2}}-\frac{1}{\sqrt{r^2+\left(z-h\right)^2}}\right]. \quad (28)$$

5. Numerical Results

5.1 Normalized Numerical Consolidation Results

The particular interest is the settlement of stratum at each stage of the consolidation process. The average consolidation ratio U is defined as following:

$$U=\frac{\text{Settlement at time } t}{\text{Settlement at end of compression}}. \quad (29)$$

The average consolidation ratio U of the saturated pervious half space can be derived as below:

$$U = \frac{2ct}{h^2 + r^2} erf\left(\frac{\sqrt{h^2 + r^2}}{2\sqrt{ct}}\right) - \frac{2}{\sqrt{h^2 + r^2}}\sqrt{\frac{ct}{\pi}} exp\left(-\frac{h^2 + r^2}{4ct}\right) + erfc\left(\frac{\sqrt{h^2 + r^2}}{2\sqrt{ct}}\right). \quad (30)$$

Figure 4 shows the average consolidation ratio U at $r/h = 0$, 1, 2, 5, and 10 for the saturated pervious half space. The figure shows that U initially decreases rapidly, and then the rate of settlement reduces. As U approaches 100% asymptotically, the theoretical consolidation is never achieved. The trend revealed in this model agrees with previous models by Sivaram and Swamee (1977) that U initially decreases rapidly, and then the rate of settlement slows down.

The profiles of normalized vertical and horizontal displacements at the ground surface $z = 0$ for different dimensionless time factor $\sqrt{ct/h^2}$ are shown in Figures 5 and 6, respectively. The ground surface reveals significant horizontal displacement. For example, Fig. 6 shows that the maximum surface horizontal displacement is around 30% of the maximum ground settlement at $r/h \approx 1.272$, which can also be found from the ratio of Eqs. (21a) and (21b).

From equations (27) and (28), the profiles of normalized excess pore water pressure $p(r,z,t)/[Q\gamma_w/4\pi kh]$ of the pervious half space at four different dimensionless time factors $\sqrt{ct/h^2}$ = 1, 2, 3, and ∞ are illustrated in Fig. 7(a)-(d), respectively. The changes in excess pore water pressure have negative value $p(r,z,t)$ which is caused by suction of groundwater withdrawal. Besides, the larger magnitude of subsidence is due to a wider region influenced by the pumping.

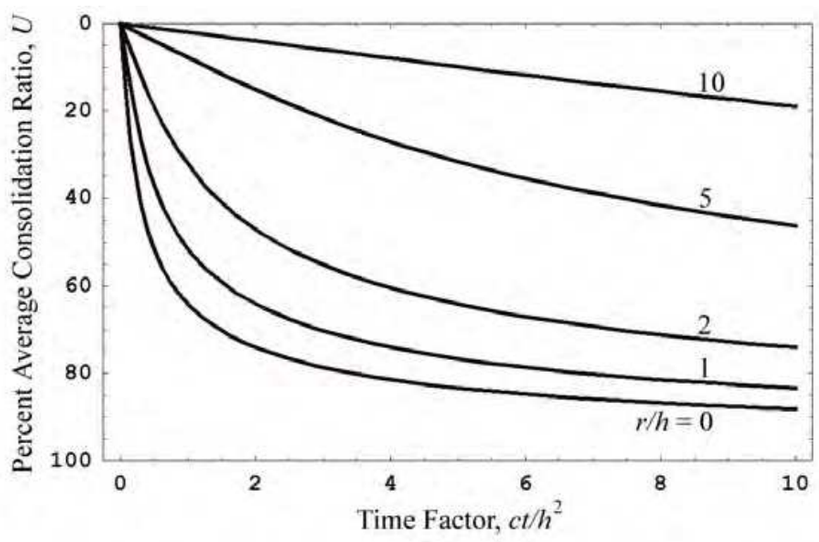

Fig. 4. Average consolidation ratio U for saturated pervious half space

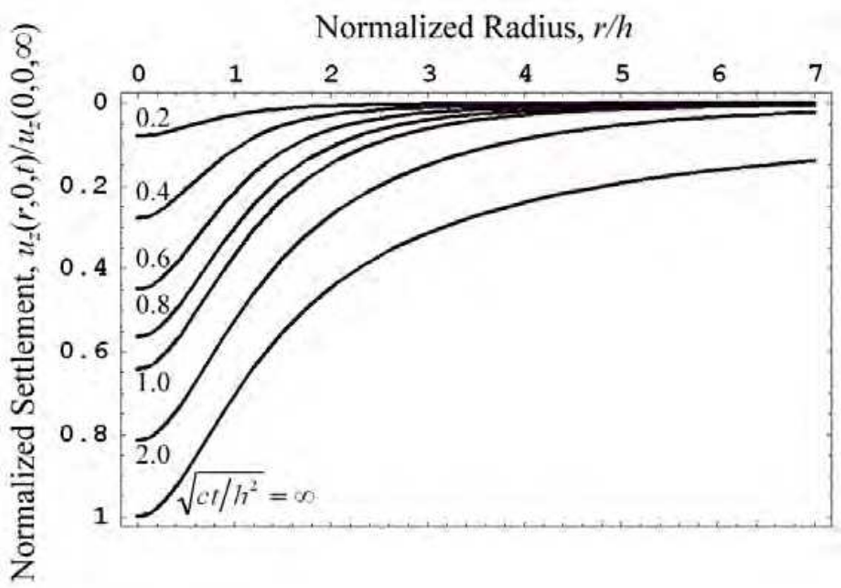

Fig. 5. Normalized vertical displacement profile at the ground surface $z = 0$ for saturated pervious half space

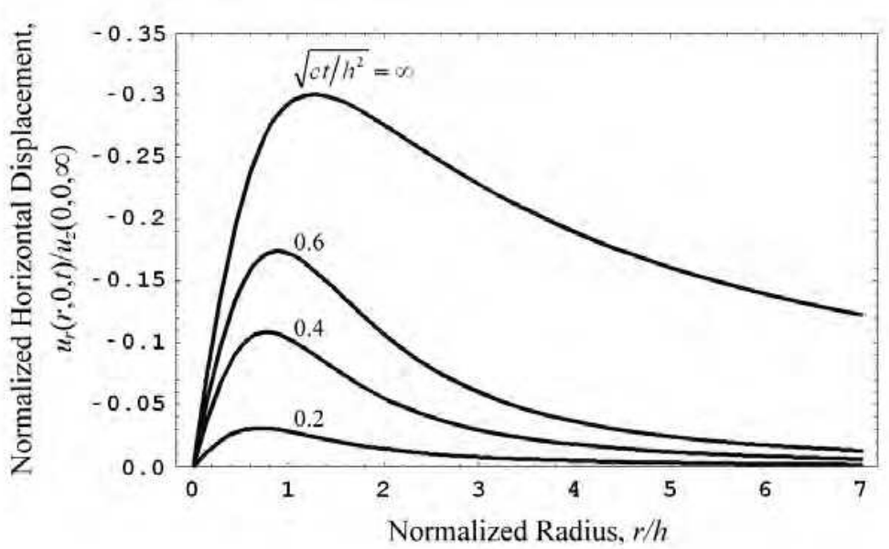

Fig. 6. Normalized horizontal displacement profile at the ground surface $z = 0$ for saturated pervious half space

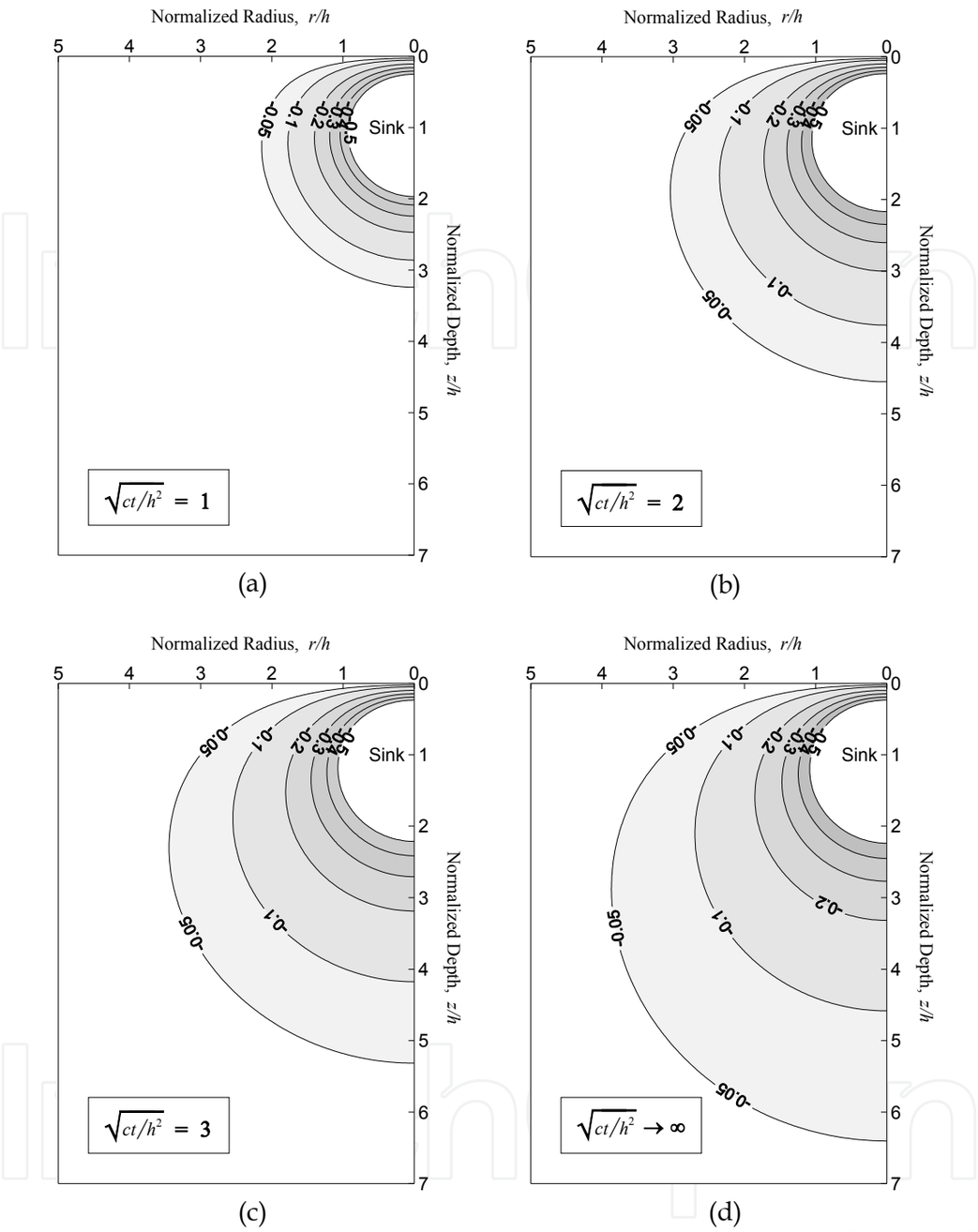

Fig. 7. Distribution of normalized excess pore water pressure $p(r,z,t)/[Q\gamma_w/4\pi kh]$ for saturated pervious half space

5.2 Practical Example

The typical values for the elastic coefficients and permeability used in the practical example of the saturated medium dense sand are listed in Table 2.

If the groundwater withdrawal can be regarded as a point sink and the pumping rate of constant strength $Q = 30\ l/s = 3\times10^{-2}\ m^3/s$, then it can have a long-term maximum horizontal

displacement and settlement at the ground surface of $1.42\,cm$ and $4.68\,cm$, respectively. It is noticed from Eqs. (21a) and (21b) that the magnitude of long-term ground surface horizontal displacement and settlement are not directly dependent on the pumping depth h of the point sink.

Parameter	Symbol	Value	Units
Shear modulus	G	20×10^{6}	N/m^2
Poisson's ratio	ν	0.3	–
Permeability	k	1×10^{-5}	m/s
Unit weight of groundwater	γ_w	9,810	N/m^3

Table 2. Typical values of the elastic properties and the permeability of a saturated medium dense sand

6. Conclusions

Closed-form solutions of the transient consolidation due to pumping from pervious saturated elastic half space were obtained by using Laplace and Hankel transformations. The study investigated the vertical and horizontal displacements of the ground surface. It also addressed the excess pore water pressure of the porous elastic half space due to a point sink. The results show:

1. The maximum ground surface horizontal displacement is around 30% of the maximum surface settlement at $r/h \approx \sqrt{\phi} = 1.272,$ where $\phi = \left(1+\sqrt{5}\right)\big/2 \approx 1.618$ is known as the golden ratio. It's interesting to find that the golden ratio ϕ also appears in the corresponding settlement of the poroelastic half space. The ground surface settlement at $r = \sqrt{\phi}h$ is around 61.8% of the maximum ground surface settlement.
2. From the average consolidation ratio U at $r/h = 0$, 1, 2, 5, and 10, it shows that U initially decreases rapidly, and then the rate of settlement reduces.
3. The magnitude of long-term maximum ground surface horizontal displacement and settlement are independent on the pumping depth h of the point sink.

7. Acknowledgements

This work is supported by the National Kaohsiung Marine University, the National Science Council of Republic of China through grant NSC97-2815-C-216-003-E, and also by the Chung Hua University under grant CHU97-2815-C-216-003-E.

8. References

Biot, M.A. (1941). General Theory of Three-dimensional Consolidation, *Journal of Applied Physics*, Vol. 12, No. 2, pp. 155-164.

Biot, M.A. (1955). Theory of Elasticity and Consolidation for a Porous Anisotropic Solid, *Journal of Applied Physics*, Vol. 26, No. 2, pp. 182-185.

Booker, J.R. & Carter, J.P. (1986*a*). Analysis of a Point Sink Embedded in a Porous Elastic Half Space, *International Journal for Numerical and Analytical Methods in Geomechanics*, Vol. 10, No. 2, pp. 137-150.

Booker, J.R. & Carter, J.P. (1986*b*). Long Term Subsidence Due to Fluid Extraction from a Saturated, Anisotropic, Elastic Soil Mass, *Quarterly Journal of Mechanics and Applied Mathematics*, Vol. 39, No. 1, pp. 85-97.

Booker, J.R. & Carter, J.P. (1987*a*). Elastic Consolidation Around a Point Sink Embedded in a Half-space with Anisotropic Permeability, *International Journal for Numerical and Analytical Methods in Geomechanics*, Vol. 11, No. 1, pp. 61-77.

Booker, J.R. & Carter, J.P. (1987*b*). Withdrawal of a Compressible Pore Fluid from a Point Sink in an Isotropic Elastic Half Space with Anisotropic Permeability, *International Journal of Solids and Structures*, Vol. 23, No. 3, pp. 369-385.

Chen, G.J. (2002). Analysis of Pumping in Multilayered and Poroelastic Half Space, *Computers and Geotechnics*, Vol. 30, No. 1, pp. 1-26.

Chen, G.J. (2005). Steady-state Solutions of Multilayered and Cross-anisotropic Poroelastic Half-space Due to a Point Sink, *International Journal of Geomechanics*, Vol. 5, No. 1, pp. 45-57.

Dunlap, R.A. (1997). *The Golden Ratio and Fibonacci Numbers*, World Scientific Publishing, Singapore, River Edge, N.J.

Erdelyi, A.; Magnus, W., Oberhettinger, F. & Tricomi, F.G. (1954). *Tables of Integral Transforms*, McGraw-Hill, New York.

Hou, C.-S.; Hu, J.-C., Shen, L.-C., Wang, J.-S., Chen, C.-L., Lai, T.-C., Huang, C., Yang, Y.-R., Chen, R.-F., Chen, Y.-G. & Angelier, J. (2005). Estimation of Subsidence Using GPS Measurements, and Related Hazard: the Pingtung Plain, Southwestern Taiwan, *Comptes Rendus Geoscience*, Vol. 337, No. 13, pp. 1184-1193.

Kanok-Nukulchai, W. & Chau, K.T. (1990). Point Sink Fundamental Solutions for Subsidence Prediction, *Journal of Engineering Mechanics*, Vol. 116, No. 5, pp. 1176-1182.

Livio, M. (2002). *The Golden Ratio: The Story of Phi, the World's Most Astonishing Number*, Broadway Books, New York.

Lu, J. C.-C. & Lin, F.-T. (2006). The Transient Ground Surface Displacements Due to a Point Sink/Heat Source in an Elastic Half-space, *Geotechnical Special Publication No. 148*, *ASCE*, pp. 210-218.

Lu, J. C.-C. & Lin, F.-T. (2008). Modelling of Consolidation Settlement Subjected to a Point Sink in an Isotropic Porous Elastic Half Space, *Proceedings of the 17th IASTED International Conference on Applied Simulation and Modelling*, Corfu, Greece, pp. 141-146.

Moorman, C.M. & Goff, J.E. (2007). Golden Ratio in a Coupled-oscillator Problem, *European Journal of Physics*, Vol. 28, pp. 897-902.

Poland, J.F. (1984). *Guidebook to Studies of Land Subsidence Due to Ground-water Withdrawal*, Unesco, Paris, France, 305 p.

Puri, P. & Jordan, P.M. (2006). On the Steady Shear Flow of a Dipolar Fluid in a Porous Half-Space, *International Journal of Engineering Science*, Vol. 44, pp. 227-240.

Sen, S.K. & Agarwal, R.P. (2008). Golden Ratio in Science, as Random Sequence Source, its Computation and Beyond, *Computers and Mathematics with Applications*, Vol. 56, pp. 469-498.

Sivaram, B. & Swamee, P.K. (1977). A Computational Method for Consolidation Coefficient, *Soils and Foundations*, Vol. 17, No. 2, pp. 48-52.
Sneddon, I.N. (1951). *Fourier Transforms*, McGraw-Hill, New York, pp. 48-70.
Tarn, J.-Q. & Lu, C.-C. (1991). Analysis of Subsidence Due to a Point Sink in an Anisotropic Porous Elastic Half Space, *International Journal for Numerical and Analytical Methods in Geomechanics*, Vol. 15, No. 8, pp. 573-592.

9. Notation of Symbols

c	Parameter, $c = k/n\beta\gamma_w$ (m^2/s)
$erf(x)/erfc(x)$	Error function/complementary error function (Dimensionless)
G	Shear modulus of the isotropic porous aquifer (Pa)
h	Pumping depth (m)
$I_v(x)$	Modified Bessel function of the first kind of order ν (Dimensionless)
$J_v(x)$	First kind of the Bessel function of order ν (Dimensionless)
k	Permeability of the isotropic porous aquifer (m/s)
n	Porosity of the porous aquifer (Dimensionless)
p	Excess pore fluid pressure (Pa)
$\tilde{p}$	Hankel and Laplace transforms of p, Eq. (12c)
Q	Pumping rate (m^3/s)
(r,θ,z)	Cylindrical coordinates system $(m, radian, m)$
s	Laplace transform parameter (s^{-1})
t	Time (s)
$u(t)$	Heaviside unit step function (Dimensionless)
u_r/u_z	Radial/axial displacement of the porous aquifer (m)
$u_{r\max}/u_{z\max}$	Maximum ground surface horizontal/vertical displacement of the porous aquifer (m)
$\tilde{u}_r/\tilde{u}_z$	Hankel and Laplace transforms of u_r/u_z, Eqs. (12a)-(12b)
β	Compressibility of groundwater (Pa^{-1})
γ_w	Unit weight of groundwater (N/m^3)
$\delta(x)$	Dirac delta function (m^{-1})
δ_{ij}	Kronecker delta (Dimensionless)
ε	Volume strain of the porous aquifer (Dimensionless)
ε_{ij}	Strain components of the porous aquifer (Dimensionless)
η	Parameter, $\eta = (1-\nu)/(1-2\nu)$ (Dimensionless)
ν	Poisson's ratio of the isotropic porous aquifer (Dimensionless)
ξ	Hankel transform parameter (m^{-1})
τ_{ij}	Total stress components of the porous aquifer (Pa)
ϕ	Golden ratio, $\phi = 1.618$ (Dimensionless)

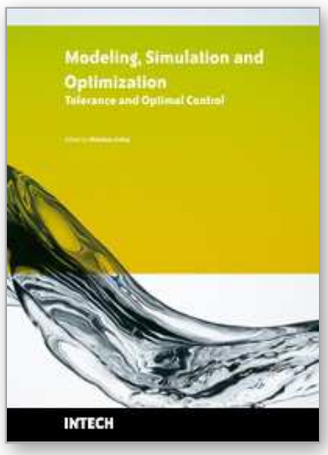

Modeling Simulation and Optimization - Tolerance and Optimal Control

Edited by Shkelzen Cakaj

ISBN 978-953-307-056-8
Hard cover, 304 pages
Publisher InTech
Published online 01, April, 2010
Published in print edition April, 2010

Parametric representation of shapes, mechanical components modeling with 3D visualization techniques using object oriented programming, the well known golden ratio application on vertical and horizontal displacement investigations of the ground surface, spatial modeling and simulating of dynamic continuous fluid flow process, simulation model for waste-water treatment, an interaction of tilt and illumination conditions at flight simulation and errors in taxiing performance, plant layout optimal plot plan, atmospheric modeling for weather prediction, a stochastic search method that explores the solutions for hill climbing process, cellular automata simulations, thyristor switching characteristics simulation, and simulation framework toward bandwidth quantization and measurement, are all topics with appropriate results from different research backgrounds focused on tolerance analysis and optimal control provided in this book.

INTECH
open science | open minds

InTech Europe
University Campus STeP Ri
Slavka Krautzeka 83/A
51000 Rijeka, Croatia
Phone: +385 (51) 770 447
Fax: +385 (51) 686 166
www.intechopen.com

InTech China
Unit 405, Office Block, Hotel Equatorial Shanghai
No.65, Yan An Road (West), Shanghai, 200040, China
中国上海市延安西路65号上海国际贵都大饭店办公楼405单元
Phone: +86-21-62489820
Fax: +86-21-62489821

IntechOpen